RSC Advances

This is an *Accepted Manuscript*, which has been through the Royal Society of Chemistry peer review process and has been accepted for publication.

Accepted Manuscripts are published online shortly after acceptance, before technical editing, formatting and proof reading. Using this free service, authors can make their results available to the community, in citable form, before we publish the edited article. This *Accepted Manuscript* will be replaced by the edited, formatted and paginated article as soon as this is available.

You can find more information about *Accepted Manuscripts* in the Information for Authors.

Please note that technical editing may introduce minor changes to the text and/or graphics, which may alter content. The journal's standard Terms & Conditions and the Ethical guidelines still apply. In no event shall the Royal Society of Chemistry be held responsible for any errors or omissions in this *Accepted Manuscript* or any consequences arising from the use of any information it contains.

ROYAL SOCIETY OF CHEMISTRY

www.rsc.org/advances

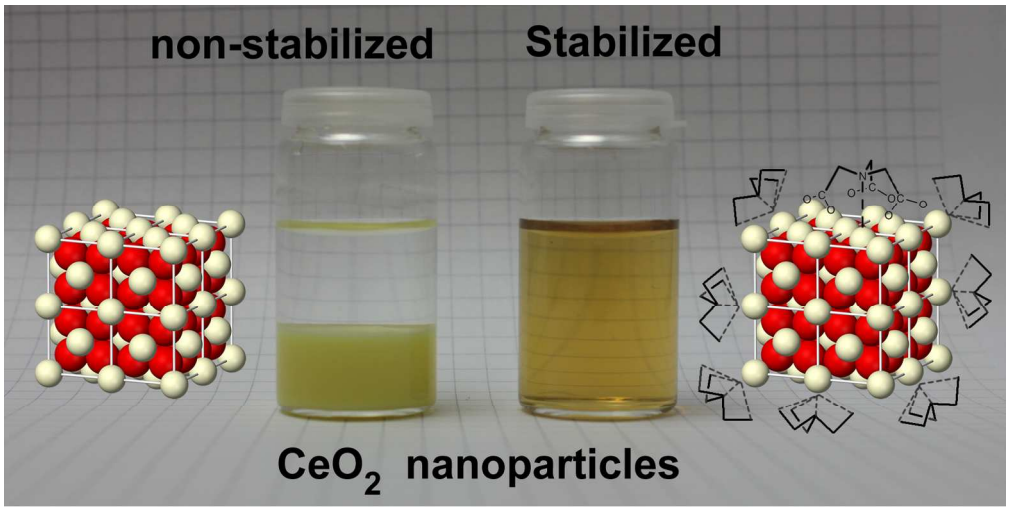

RSC Advances Accepted Manuscript

Aminopolycarboxylic Acids as a Versatile Tool to Stabilize Ceria Nanoparticles – A Fundamental Model Experimentally Demonstrated

Eric Johansson Salazar-Sandoval[†,‡], Mats K.G. Johansson[‡], Anwar Ahniyaz[†,*]

[†]SP Technical Research Institute of Sweden, Chemistry, Materials and Surfaces, Box 5607, SE-114 86 Stockholm, Sweden

[‡]Department of Fibre and Polymer Technology, School of Chemical Science and Engineering, KTH Royal Institute of Technology, SE-100 44 Stockholm, Sweden

* Corresponding author

An extremely stable water dispersion of cerium oxide nanoparticles was prepared by colloidal synthesis, using nitrilotriacetic acid (NTA) as a stabilizer. Based on FT-IR measurements, the surface characteristics of NTA-stabilized ceria nanoparticles are clarified and a fundamental stabilization mechanism is proposed. The mechanism is based on the combination of the ionic nature of cerium oxide surface and the inner-sphere complexation model. From an application perspective it is remarkable that ceria nanoparticle dispersions stabilized by NTA are stable at neutral pH, which makes them a potential successful additive in UV screening applications.

Keywords: aminopolycarboxylic acid, nitrilotriacetic acid (NTA), cerium oxide, nanoparticles, aqueous dispersion

Introduction

Cerium oxide (CeO_2) nanoparticles has attracted great interest in many industries due to their applications[1] in chemical mechanical planarization[2], as diesel fuel additive,[3] in fuel cells[4] and as UV

RSC Advances Accepted Manuscript

screening additives for coating[5] and cosmetics[6]. Due to the environmental and toxicological concern on safe handling of cerium oxide nanopowders, stable suspensions of the nanomaterials in various liquids are needed and preferred for practical applications. Due to the strict volatile organic compound (VOC) emission control, aqueous dispersion of cerium oxide nanoparticles is preferred by the industry, over the organic solvent dispersion. Ceria nanoparticles have been incorporated in clear coatings to protect wood from UV-induced degradation of lignin.[7, 8] The main challenge was to obtain stable water dispersion of cerium oxide nanoparticles that is compatible with commercially available waterborne clear coatings. Without having access to non-aggregated cerium oxide nanoparticle water dispersion, it is not possible to use it in clear coating formulation as UV-absorber. In sunscreen cosmetic application, it is also important to have access to colloidal dispersion of ceria.[9, 10] For chemical mechanical planarization (CMP) applications, it is desired to have highly stable dispersion of cerium oxide nanoparticles to polish semiconductors.[11, 12] Without having stable dispersions of ceria, it is not possible to achieve high efficiency.[13, 14] In catalyst production, ceria nanoparticles need to be incorporated into other matrix in close contact with noble metal nanoparticles to improve efficiency of the catalyst.[15] Stable dispersion of ceria nanoparticles is required to assure the consistency and homogenous of the catalyst.[1] Well dispersed ceria nanoparticles provide high surface area and high oxygen storage capacity as well.[16] In diesel fuel additive application, it is important to have a stable colloidal dispersion of ceria nanoparticles in the fuel. Unstable dispersion would lead to phase separation, thus affect the efficiency during combustion.[17, 18] In fuel cell applications, well dispersed ceria nanoparticles are required in the production of highly efficient electrodes.[19]

Thus, there is an increasing need for the aqueous dispersion of cerium oxide nanoparticles that is stable at neutral pH. Both solid content and storage stability of the dispersions are often critical for practical applications.

RSC Advances Accepted Manuscript

In the past, numerous studies have been carried out to obtain stable aqueous and non-aqueous suspension of cerium oxide nanoparticles. Some examples are the oleate–stabilized ceria nanorods prepared by Ahniyaz *et al*.[20]; the citrate–stabilized ceria nanoparticles reported by Masui and coworkers[21] and the nanoparticles stabilized with poly(acrylic acid) prepared by Sehgal *et al*.[22]

Both surface area and surface chemistry of nanoparticles are important in stabilization and dispersion of nanoparticles in a certain liquid medium. When the particle size is reduced, inevitably, on the surface, the crystal lattice is disrupted causing an incomplete coordination, which explains the high reactivity of nanoparticle surfaces in general. This gives rise to a surface tension that strives to be reduced in different ways. One route would be to reduce the valence of surface atoms. In agreement with Wertheim,[23] Johansson[24] and Schweda,[25] the surface of bare ceria must be anticipated to consist, to some extent, of trivalent cerium. Another possibility is to grow in size, while not reducing the valence; thus the number of valently unsaturated atoms decreases in number. For ceria dispersions in solution, Ostwald ripening is a consequence of this phenomenon. A different alternative is the adsorption of other molecules or compounds capable of satisfy, or saturate, the uncoordinated valence.[26] A particular and fatal case of this last occurrence, when particles are dispersed in solution, is the adsorption of a second nanoparticle, which leads to aggregation. It is our understanding that these three phenomena (reduction of surface valence, Ostwald ripening and adsorption) have a great effect on the dispersion stability and size distribution of cerium oxide nanoparticles in aqueous system.

To achieve a stable dispersion, the chemist is left with the single alternative of finding an adequate stabilizer that, when adsorbed, fulfills the coordination needs of surface atoms, thus minimizing the surface tension while, at the same time, allows for a kinetically stable dispersion to be formed. In the present study we investigate whether a chelating agent, known to complex a free metal cation, is able to

RSC Advances Accepted Manuscript

form a surface complex on the corresponding metal oxide nanoparticles. To confirm the assumption, it is required that a chelating agent stabilizes a nanoparticle dispersion of the metal oxide in aqueous solution. In the present study, we have focused our efforts on the pair cerium oxide / nitrilotriacetic acid (NTA); because NTA is known to be an excellent sequestering agent for trivalent cations and has been employed in the separation of the different rare earth metals.[27, 28]

Experimental Details

Materials and synthesis:

Cerium (III) nitrate hexahydrate, Ammonium hydroxide solution, (28.0-30.0%) Nitrilotriacetic acid (98+% ACS reagent) [Scheme 1] and Sodium nitrilotriacetate (Sigma-grade) were purchased from Sigma-Aldrich. Hydrogen peroxide 30% was purchased from MERCK. Double distilled water was used for all the experiments.

Scheme 1. NTA

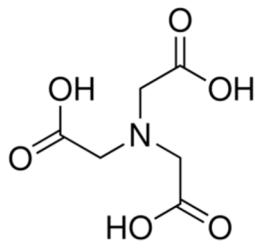

Representation of the nitrilotriacetic acid (NTA) molecule

Neutralization of the stabilizer

RSC Advances Accepted Manuscript

6 grams of NTA were added to 100 mL of H_2O and while stirring, NH_4OH solution was added dropwise until complete dissolution of the acid.

Synthesis of cerium oxide (ceria) nanoparticles

In a typical synthesis procedure, 30 grams of $Ce(NO_3)_3 \cdot 6H_2O$ were added to 400 mL H_2O and stirred until complete dissolution. Then, 22 grams of NH_4OH solution were added (pH raised to ca. 9.7) and the precipitate was collected by centrifugation to obtain a wet cake. Afterwards, the wet cake was re-dispersed in 2 L of pre-heated (at 80 °C) hot water, using a mechanical disperser, Ultra-Turrax (IKA Works GmbH, Germany) at 10,000 rpm. Then the temperature was raised to 88 °C and continuously stirred with Ultra-Turrax. After re-dispersion, the previously prepared neutralized-NTA solution was added to the reaction batch and left stirring for another 15 minutes. After that, 8 grams of H_2O_2 solution were added to oxidize Ce^{3+} to Ce^{4+}. The suspension was continuously stirred with Ultra-Turrax for one more hour at 88 °C.

One hour after the addition of the peroxide, the Ultra-Turrax stirring and heating plate were turned off and left for cooling down, under magnetic stirring, to obtain stable aqueous dispersion of NTA-stabilized cerium oxide nanoparticles. pH and conductivity of the dispersion were measured as 6.8 and 7.4 $mS \cdot cm^{-1}$, respectively.

Synthesis of cerium nitrilotriacetate

Equimolar quantities of $Ce(NO_3)_3 \cdot 6H_2O$ and Na_3NTA were reacted together to obtain Ce(NTA).

43.44 grams of $Ce(NO_3)_3 \cdot 6H_2O$ and 25.72 grams of Na_3NTA were dissolved in separate beakers with double distilled water and aided by magnetic stirring. Upon complete dissolution, the two solutions were mixed together and resultant precipitate was collected by centrifuging at 4000 rpm for 20 minutes. The

RSC Advances Accepted Manuscript

precipitate, Ce(NTA), was washed with abundant water and centrifuged. This was repeated twice to eliminate impurities of sodium, nitrates and unreacted reagents. Finally, it was dried at 50 °C in vacuum oven overnight.

Freeze drying of cerium oxide nanoparticle dispersions

Drying the cerium oxide nanoparticles dispersion was necessary for later characterization by ATR-FTIR as described below. Dispersions were frozen at ca. 188 K and then transferred to a Freeze-drying apparatus where vacuum levels of ca. 2 Pa were maintained for 48 hours. The freeze-drying technique was chosen over conventional oven or vacuum oven because it minimizes the aggregation of nanoparticles that is likely to occur during the evaporation of water.

Characterization techniques

FT-IR

A PerkinElmer Fourier Transform Infrared (FT-IR) -Spectrometer, Spectrum One with Attenuated Total Reflection (ATR) sampling accessory was used with a MIR (mid-infrared) beam source. The instrument is equipped with KRS-5 and diamond ATR crystals on the top plate and with a MIR-DTGS (mid-infrared deuterated tryglycine sulfate) detector. A few milligrams of sample were placed directly on the ATR crystal. Spectra were recorded with 16 scans and a resolution of 2 cm^{-1}.

DLS

Particle size distribution was analyzed by Dynamic Light Scattering (DLS) using a Zetasizer (Nano ZS, 2003, Malvern Instruments, UK). The measurement angle was 173° (backscatter). Both, the standard

RSC Advances Accepted Manuscript

general purpose algorithm and the so-called high resolution mode were used for the analyses. Disposable plastic cuvettes were used once per measurement.

An aliquot of the dispersion was diluted with double-distilled water and the diluted sample was then analyzed by DLS.

TEM

Low and high resolution Transmission Electron Microscopy (TEM) images were obtained using a JEOL JEM-3010 microscope operating at 300 kV (Cs = 0.6 mm, Point resolution 0.17 nm). Images were recorded with a CCD camera (MultiScan model 794, Gatan, 1024 x 1024 μm) at a magnification of 4,000 – 800,000X. TEM samples were prepared by diluting the ceria dispersion in water 200 times and applying a drop onto the copper side of a carbon coated Cu grid. The water was allowed to slowly evaporate at room temperature.

UV-Vis

UV-Vis spectra of the samples were collected with a Perkin Elmer Lambda-650 spectrometer. Two light sources were used: deuterium lamp between 250 and 218 nm and tungsten lamp between 218 and 600 nm. Plastibrand disposable UV-cuvettes with 1 cm of optical path length were used for each measurement and its corresponding background. Single scan spectra were recorded with a resolution of 1 nm.

TGA

RSC Advances Accepted Manuscript

To quantify the cerium oxide content of the dispersions, thermogravimetry analyses (TGA) were carried out in a Perkin-Elmer TGA analyzer. The temperature was set to increase from 25 °C to 800 °C at the rate of 20 °C·min^{-1}.

XRD

X-ray diffraction (XRD) analysis was carried out to verify the crystal structure of the NTA-stabilzied cerium oxide nanoparticles.

XRD analysis was performed using an Agilent Xcalibur III single-crystal diffractometer with a 4-circle kappa geometry, equipped with Sapphire 3 CCD detector and Molybdenum radiation source. On the diffractometer a capillary containing the NTA-stabilized ceria dispersion was mounted, and the 2D-data were converted and merged to a conventional powder diffraction pattern.

XPS

X-ray photoelectron spectroscopy (XPS) studies were conducted to verify the valence of surface cerium in the obtained NTA-modified CeO_2 nanoparticles.

The spectra were recorded using a Kratos AXIS Ultra^{DLD} X-ray photoelectron spectrometer (Kratos Analytical, Manchester, UK). The sample was analyzed using a monochromatic Al X-ray source. The analysis area was below 1 mm^2, with most of the signal from an area of 700 x 300 μm.

Results and discussion

A model for stabilization of nanoparticles based on the inner-sphere complexation model.

The complexes formed between cerium ions and organic ligands have previously been extensively investigated.[27, 29] According these studies, cerium (III) and (IV) ions are classified as hard acids, as

RSC Advances Accepted Manuscript

defined by Pearson,[30] because they are relatively small and highly charged. Therefore, they bond to electron donors, preferably to those small and difficult to polarize; also known as hard bases of Pearson. Examples of hard bases are fluorine and oxygen ions. Bonding between hard acids and bases is predominantly ionic.[30]

Among the different organic functional groups, the carboxylate provides a supreme electron donor environment for complexing hard Pearson acids, i.e. carboxylates are excellent hard bases of Pearson. The hard donor character of the carboxylate is the source for ionic bonding with lanthanide cations as also reflected on the rapid kinetics of complexation.[31] For carboxylic acids, the logarithm of the formation constant (log β) is proportional to the sum of the pK_a, which provides additional evidence supporting the ionic nature of the metal-ligand interaction.[32]

If carboxylic acids act as ligands through their carboxylate groups, one could expect to find differences between these ligands depending on their acidity. In water, acidity can be seen as a tendency to deprotonate, transferring the proton to a conjugated pair. Thus, solvating the recently formed ions and consequently placing water molecules between them, which precisely, leads to two kinds of complexes: inner-sphere and outer-sphere complexes. As exemplified in Figure 1, inner-sphere complexes are those where the ligand is in direct contact to the metal ion.[33] On the contrary, in the outer-sphere complexes one or more layers of water of hydration remain between the metal ion and the ligand.[34]

RSC Advances Accepted Manuscript

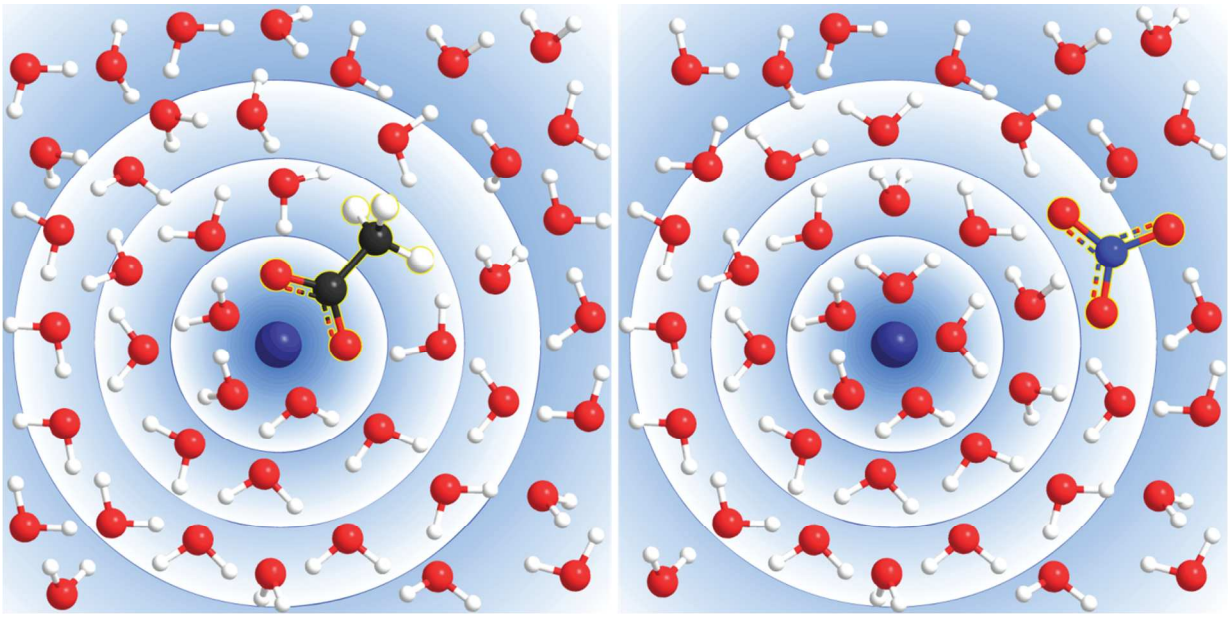

Figure 1. The acetate inner-sphere complex, in direct contact with the hydrated central cation (left); and the nitrate outer-sphere complex separated by several hydration layers from the central cation (right).

Inner-sphere complexes are more stable than outer-sphere and the stability is explained as an increase in entropy.[35] Disruption of the hydration shell is an endothermic reaction that requires an amount of energy which is not regained by formation of the —lower in number— exothermic interactions between the metal and the ligand. As a result, the net reaction tends to be endothermic. However, breaking the hydration shell releases enough number of water molecules to increase the entropy to upset the balance towards negative values of ΔG i.e. a favorable reaction.[33]

Inner-sphere complexation –in water– implies breaking several strong ionic M^{n+}–O bonds, formed between the metal ion and solvating water (H_2O–M^{n+}); and the formation of another strong ionic bond[36] between the metal and its ligand (e.g. R-CO_2–M^{n+}). That is, ligands forming inner-sphere complexes, replace water or hydroxyl groups when binding a metal ion.

Two different approaches have been developed to discern between the carboxyl group of a carboxylic acid interacting in an outer- or inner-sphere fashion. The first of these methods refers to the pK_a of the

RSC Advances Accepted Manuscript

acid. It was concluded that for acids with a pK_a <2 the behavior is outer-sphere, while for pK_a >3 the inner-sphere predominates; and for 2< pK_a <3 an intermediate situation occurs[37]. The second method accounts for the magnitude of ΔS for the complexation reaction[38]. Taking as a reference lanthanum acetate, ΔS = 67 $J \cdot mol^{-1} \cdot K^{-1}$ and assuming completely inner-sphere interaction; and lanthanum trichloroacetate ΔS = 0 for completely outer-sphere behavior; Huskens and coworkers could easily calculate a 91% and 51% inner-sphere value for lanthanum acrylate (ΔS = 61 $J \cdot mol^{-1} \cdot K^{-1}$) and propanoate ($\Delta S$ = 34 $J \cdot mol^{-1} \cdot K^{-1}$), respectively.

From the above discussion it follows that the higher the pK_a value of a carboxylic acid, the more inner-sphere behavior and hence, the more stable the complex. If so, glycolic acid, which is a stronger acid than acetic, would lead to less stable complexes. Quite the opposite, glycolate complexes are, in general, more stable than those of acetic and the increased stability is attributed to chelation[39]. In fact, when in 1937, Diehl first defined chelates as ligands bonding through more than one point, he already pointed out chelates provide increased stability.[40] Later, in 1952, Schwarzenbach[41] demonstrated the nature of the chelate effect using as models one bidentate ligand and two monodentate ligands which form coordinate bonds of equivalent strength with a metal ion. Since the heat of reaction was kept close to zero i.e. $\Delta H \approx 0$ the greater stability accomplished was thought to be an entropic effect. There is now clear evidence that the increment in entropy $-\Delta S-$ is proportional to the number of carboxyl groups in the ligand.[42-44] For instance, ΔS for the complexation of Ce(III) with NTA[44] is about 180 $J \cdot mol^{-1} \cdot K^{-1}$, which is three times higher than that for acetate: 60 $J \cdot mol^{-1} \cdot K^{-1}$. The higher stability of chelates is interpreted as the result of being more favorable to bond the second, and subsequent, donor units of the multidentate ligand to the metal ion, once the first unit is already bonded; compared bonding more than one molecule of monodentate ligands.[45] Besides, the difference in entropy between chelates and monodentate ligands is also interpreted as a consequence of the change in the number of species before

RSC Advances Accepted Manuscript

and after the reaction[46]. Tridentate chelates for instance would have two less molecules in the reactants compared to three monodentate ligands. In addition, chelates usually release more water molecules from the hydration shell of the metal compared to monodentate ligands.[33]

The present study proposes a model to explain the formation of surface complexes of aminopolycarboxylic acids on metal oxides and its consequence in formation and stabilization of metal oxide nanoparticles. Further, the generic model described is experimentally verified with the ceria / NTA pair.

Making use of the knowledge we have just reviewed, the potential of NTA as chelating agent for cerium ions is clearly exposed: it has multiple electron donor units –the three carboxylates–, therefore it benefits form a chelate effect; in addition, it forms inner-sphere complexes. Previously reported[44] ΔS value for the complexation reaction between cerium and nitrilotriacetic acid is 180 $J \cdot mol^{-1} \cdot K^{-1}$ and, as reviewed above, entropy involved in inner-sphere complexation of one carboxylate group lies in the 60 $J \cdot mol^{-1} \cdot K^{-1}$ range. Therefore, having three carboxylates in NTA, and being the main responsible for the entropy change in the reaction, indicates inner-sphere complexation for cerium nitrilotriacetate in aqueous solution. This is in agreement with the models by Gfeller[47] and the structures proposed by Nakamoto.[48]

The literature describes, thus, a cerium nitrilotriacetate molecule resembling the one presented in Figure 2: the metal ion is coordinated to the three carboxylate groups by ionic interactions and to the nitrogen atom in NTA by dative covalent bonding.[49] Our model, Figure 3, would be made up of a ceria surface with cerium atoms exposed and NTA forming a surface complex of similar interactions to those found in Ce(NTA).

RSC Advances Accepted Manuscript

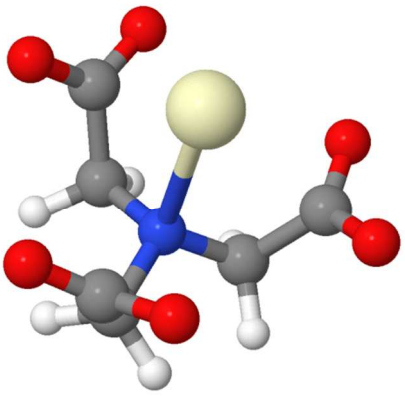

Figure 2. Representation of the cerium (III) nitrilotriacetate complex. The bond between the nitrogen atom (blue) and the cerium ion (beige) is shown to enhance spatial visualization and understanding. There is also bonding between cerium and the oxygen atoms (red) of the carboxylates. These bonds are not shown because they are ionic and therefore not spatially oriented.

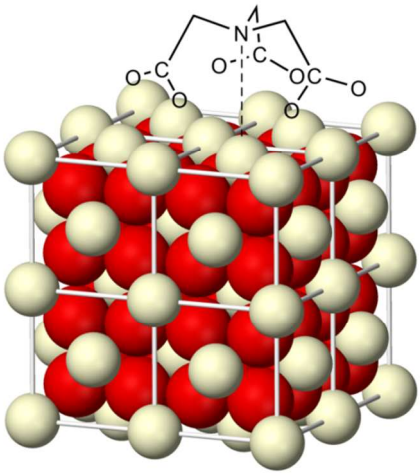

Figure 3. Surface complex formed by the NTA molecule coordinated on the surface of crystalline ceria according to our model (oxygen and cerium ions in red and beige, respectively).

To extend the Ce(NTA) model to CeO_2-NTA system we shall also provide solid grounds for equating the reactivity towards NTA of both the aquatic Ce ions and the surface of CeO_2.

RSC Advances Accepted Manuscript

Chemical properties and reactivity are always based on the electronic structure of atoms and compounds, thus it is of great importance understanding that cerium oxides consist of ions hold together by polarized ionic bonding.[50] In aqueous solution, the surface of ceria also adopts a mixed valence state. To support this argument we find conclusive Morss'[51] values of ΔG for the reaction CeO_2 to Ce_2O_3 which indicates that in bulk the most stable form is CeO_2; while in solution, thermodynamics reveal that the trivalent cation is the stable species. Therefore, surface cerium atoms exposed to water would find a more comfortable (less aggressive) environment in their trivalent state. Interestingly, ΔG values for the reactions $CeO_2(s) \rightarrow CeO_{1.5}(s) + ¼O_2(g)$ and $Ce^{4+}(aq) + e^- \rightarrow Ce^{3+}(aq)$ are –in absolute terms– rather similar (172 vs. -166 kJ·mol^{-1}, respectively), supporting the proposed ability for the cerium ion to adjust its charge in order to minimize the energy of the system it belongs to. All this literature is brought here to present the reader that cerium oxides are ionic lattices to which NTA can interact on the surface, as it would do with the aquatic cerium ions.

Experimental validation of the proposed model

- **Spectroscopic validation of the model**

X-ray studies validate our synthetic strategy by confirming that we obtained the typical diffraction pattern of the cubic fluorite structure with $Fm\bar{3}m$ space group. Further, the observed diffraction pattern matches the calculated pattern for the ceria structure with unit cell of ca. 5.42 Å (see Supplementary Information for details on synthetic strategy and x-ray diffractions results. Please, note that molybdenum radiation was used).

It is well known that the frequency of vibration of the carboxylate group varies when it is protonated, deprotonated or bonded to a metal atom. Moreover, the vibration frequency depends on the metal to

RSC Advances Accepted Manuscript

which the acid is associated.[52] FT-IR studies, Figure 4, of the protonated nitrilotriacetic acid, NTA (notated in the figure as H_3NTA to emphasize the acid is protonated) and the cerous nitrilotriacetate, Ce(NTA) shows that the carboxylate asymmetric vibration band (ν_{as}) shifts from 1713 to 1579 cm^{-1} when cerium (III) replaces the three protons. Similarly, the FT-IR spectrum of CeO_2-NTA shows a band for the carboxylate asymmetric vibration (ν_{as}) at 1568 cm^{-1}; result that we interpret as evidence that the NTA is interacting with cerium ions on ceria surface in a similar fashion to that of Ce(NTA) and thus confirming experimentally that NTA forms a surface complex. Interestingly, the carboxylate ν_{as} value of 1568 cm^{-1} observed here coincides with that previously reported for the adsorption of citrate on ceria[53]. Furthermore, the surface of hydrated ceria has been argued to consist, to some extent, of trivalent cerium and thus, the similarity between the surface complex CeO_2-NTA and the chelate Ce(NTA), in terms of the infrared results presented here, can be comprehended. In order to verify experimentally that substantial amount of Ce (III) can be found on the surface of the NTA-stabilized CeO_2 nanoparticles we have conducted X-ray Photoelectron Spectroscopy (XPS) studies (results in Supplementary Information) and they show that both Ce (III) and Ce (IV) are present on the surface. However, the relative intensities of the peaks corresponding to the different oxidation states evidence that the predominant species is Ce (III).

RSC Advances Accepted Manuscript

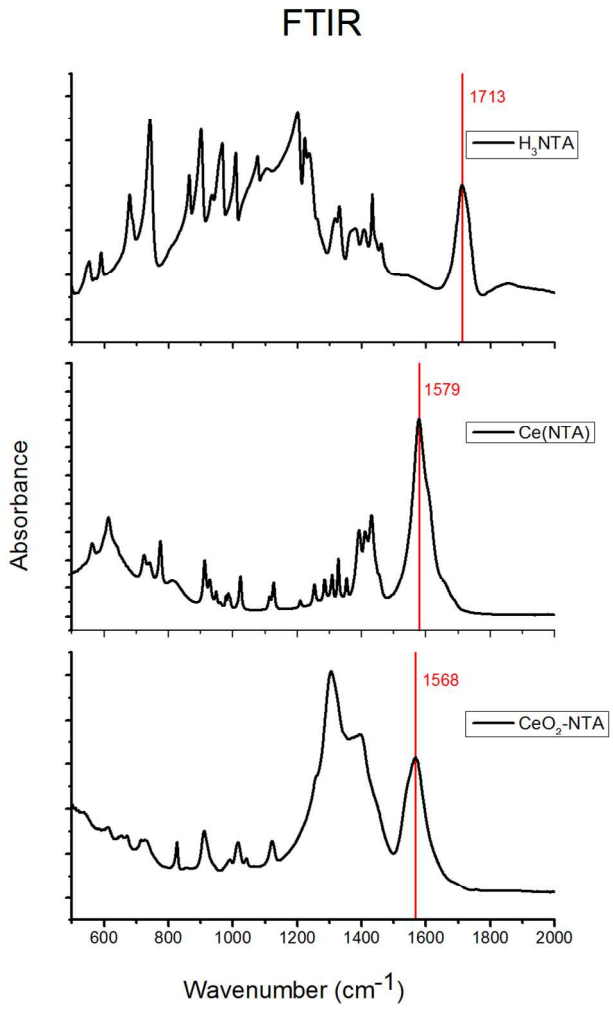

Figure 4. FT-IR of the fingerprint region of NTA (top), Ce(NTA) chelate (middle) and CeO_2-NTA system (bottom) where the carboxylate band is highlighted with accompanying values: 1713 cm^{-1} for NTA, 1579 cm^{-1} for Ce(NTA) and 1568 cm^{-1} for CeO_2-NTA.

Additionally, the nitrilotriacetate surface complex on ceria keeps particles well dispersed in aqueous solution, preventing aggregation. Hence, NTA acts as stabilizer of these nanoparticles, in fact, as an extremely good stabilizer judged by the small size of the particles obtained and the long term stability achieved.

RSC Advances Accepted Manuscript

Dispersion characteristics

The dispersion has been characterized by DLS and TEM to illustrate the small particle size obtained. The stability of the system was furthermore assessed by comparing the DLS results after 3 and 6 months of storage.

The particle's hydrodynamic radius together with the polydispersity of the sample was determined using Dynamic Light Scattering (DLS) size measurements. A comparison of the DLS results of the dispersion after 3 and 6 months of storage, Figure 5a, shows that the dispersion remains unchanged within the error of the measurement; with maximums for the 3 and 6 months curves at 16 nm. Processing the data from the DLS size measurement in the *Multiple Narrow Modes (high resolution)* settings instead of in the *General Purpose Algorithm (normal resolution)*, splits the curve in two narrower bands that better represent the actual sizes of the dispersed particles, Figure 5b. Hence, the high resolution analysis of the DLS of the dispersion after 6 months of storage displays two populations, 13 and 34 nm, Figure 5b. The smallest particles form the densest population, followed by a residual population which corresponds to sizes three times larger than the smaller group, suggesting that the larger population might arise from the aggregation of primary particles.

RSC Advances Accepted Manuscript

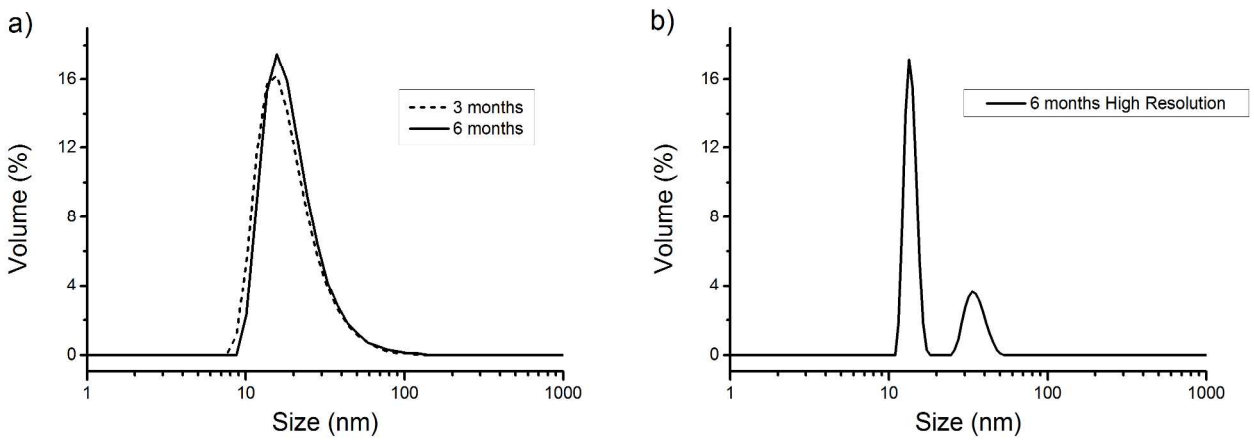

Figure 5. Particle size distribution of aqueous dispersion of NTA-stabilized CeO_2 nanoparticles measured by Dynamic Light Scattering, a) three and six months after synthesis, using the general purpose algorithm; b) six months after synthesis measured in high resolution mode.

Transmission electron microscopy (TEM) images, taken nine months after synthesis, evidence the primary particle size of cerium oxide nanoparticles is preserved in the range of 3 to 5 nm for such a long period of time, Figure 6. It is also clear from the figure that a certain degree of aggregation occurs. Whether these aggregates are present in the original dispersion or formed during the sample preparation (aggregation while drying on the TEM grid) cannot be inferred from the TEM micrographs, but certainly DLS comes to determine that aggregates up to 50 nm might be present in the dispersion, while larger ones are more likely to be originated upon drying.

RSC Advances Accepted Manuscript

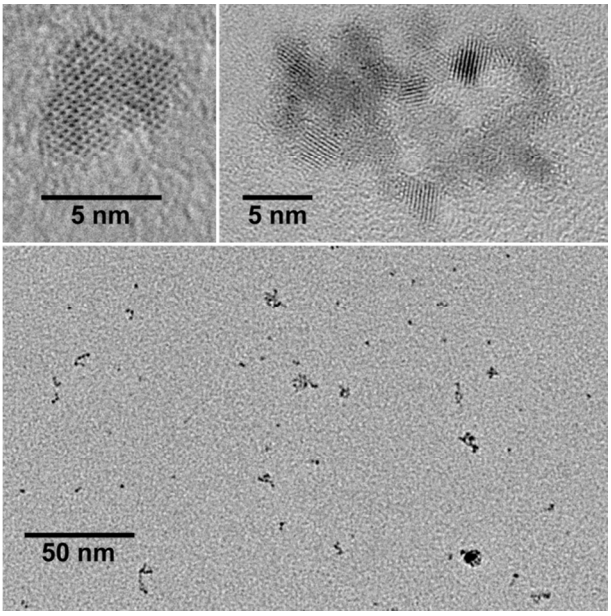

Figure 6. TEM images of the diluted and dried ceria dispersion, showing: an even distribution of particles on the TEM grid and the absence of high order aggregates (bottom); primary particle size of ca. 5 nm (top left); example of the largest aggregates of ca. 22 nm (top right).

UV-Vis spectrometry of a diluted aliquot of the NTA- stabilized cerium oxide nanoparticle dispersion is presented in Figure 7. The obtained dispersion, due to its ceria content, absorbs UV light with maximum absorption around 280 nm. Yet not colorless, it has a bronze color, shows a high degree of transparency in the visible range. Transparency, or lack of significant scattering, has its origin in the small ceria particle size attained during synthesis and maintained over time thanks to the stabilization of the nanoparticles by the NTA.

RSC Advances Accepted Manuscript

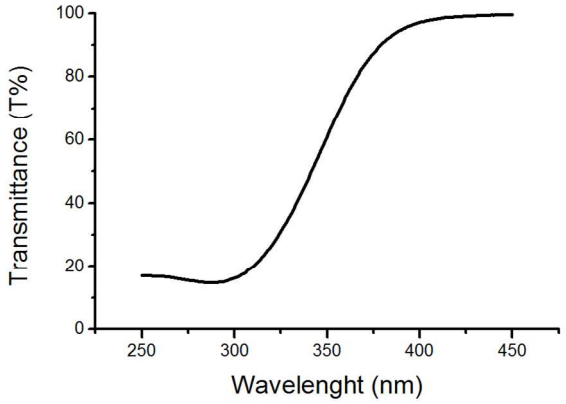

Figure 7. UV-Vis spectra, 3 months after synthesis, of a diluted aliquot of the NTA-modified ceria dispersion.

Potential applications

Due to the transparency in the visible range and long term stability of the prepared dispersions, they can find a direct application as a UV screening additive to clear coatings.[6, 54] Acrylic latexes in waterborne formulations consist of polymer particles stabilized in water by surfactants and their stabilization mechanism is very sensitive to changes in pH and ionic strength.[55, 56] The present ceria nanoparticle dispersion is attractive and suitable for use as a UV absorbing nano-additive for a UV-protective clear coating application because it is stable around neutral pH range, which is typical of acrylic latex formulation.[57]

Predictions and limitations of the model

Our model takes as subject of study an ionic lattice, ceria and an established complexing agent for cerium cations. The electron deficiency (acidity) of the cation is well balanced by the electrondonor ability (basicity) of the carboxylate groups in the complexing agent, nitrilotriacetic acid or shortly NTA.

RSC Advances Accepted Manuscript

If our model could be extended to systems other than ceria/NTA it would be intuitive to think that for the specific acidity of the different cations the best surface complex would be formed with ligands that could provide enough electron density to satisfy the uncoordination of the surface cations on the particle. Excess in providing electron density by the most basic ligands, such as the carboxylic function, could result in unsuccessful stabilization of nanoparticles if the metal is not acidic enough.

One major limitation to this model is the fact that the acid-basic interaction between the cation on the surface of the metal oxide and the ligand is only valid for ionic systems. When the nanoparticle is built on covalent bonding such as in silica, the stabilizer should be covalently bonded to the surface and a model based on finding ionic balance between surface cation and ligand as well as concepts like the inner-sphere complexation model shall no longer be applied.

Conclusion

Ultra-stable aqueous dispersion of cerium oxide nanoparticle was developed by using a chelating agent, NTA (an aminopolycarboxylic acid), as a stabilizer. The experimental results confirm our initial assumption/hypothesis that a high efficient chelate for given metal shall also work as surface complex on the associated metal oxide nanoparticle and further reveals details on the stabilization mechanism and the importance of coordination effects. Hence, the study demonstrates a versatile route to synthesize and stabilize cerium oxide nanoparticles, obtaining stable dispersions that are of interest to industry in the development of, for instance, UV screening coatings.

The ionic interaction not only explains the properties of cerium oxides but it is the key to understand the mechanism of the stabilization as we propose it. Although stabilization effect of NTA was only demonstrated for cerium oxide nanoparticles, these findings and proposed model add a new toolbox in

RSC Advances Accepted Manuscript

designing and tailoring surface functionalities/properties of metal oxide nanoparticles and their subsequent stabilization in aqueous system.

Acknowledgments

This research was funded by the EU FP7, grant agreement number 246434, WoodLife: Extended service life and improved properties of wood products through the use of functional nanoparticles in clear coating and adhesive systems. The authors wish to thank the project partners for useful discussions. The authors would also like to acknowledge Professor Dr. Lars Eriksson at the Department of Materials and Environmental Chemistry at Stockholm University for the assistance on X-ray data collection and diffraction analyses of cerium oxide nanoparticles dispersion.

References

1. C. Sun, H. Li and L. Chen, *Energy & Environmental Science*, 2012, **5**, 8475-8505.
2. J. B. Hedrick and S. P. Sinha, *Journal of Alloys and Compounds*, 1994, **207–208**, 377-382.
3. *GB Pat.,* 2004-GB3298, 2004.
4. A. Evans, A. Bieberle-Hütter, J. L. M. Rupp and L. J. Gauckler, *Journal of Power Sources*, 2009, **194**, 119-129.
5. A. Saadat-Monfared, M. Mohseni and M. H. Tabatabaei, *Colloids and Surfaces A: Physicochemical and Engineering Aspects*, 2012, **408**, 64-70.
6. T. Masui, M. Yamamoto, T. Sakata, H. Mori and G.-y. Adachi, *Journal of Materials Chemistry*, 2000, **10**, 353-357.
7. S. Bardage, M. Henriksson, S. Olsson, P. Collins, D. Meng, A. Ahniyaz, E.-J. Salazar-Sandoval, A. Rahier, M. Gasparini and N. Lamproye, *Surface Coatings International*, 2013, 2-6.
8. , 2009-2013.
9. S. Yabe and T. Sato, *Journal of Solid State Chemistry*, 2003, **171**, 7-11.
10. B. Faure, G. Salazar-Alvarez, A. Ahniyaz, I. Villaluenga, G. Berriozabal, Y. R. D. Miguel and L. Bergström, *Science and Technology of Advanced Materials*, 2013, **14**, 023001.
11. Y. Ein-Eli and D. Starosvetsky, *Electrochimica Acta*, 2007, **52**, 1825-1838.
12. X. Feng, D. C. Sayle, Z. L. Wang, M. S. Paras, B. Santora, A. C. Sutorik, T. X. T. Sayle, Y. Yang, Y. Ding, X. Wang and Y.-S. Her, *Science (Washington, DC, United States)*, 2006, **312**, 1504-1508.

RSC Advances Accepted Manuscript

13. P. B. Zantye, A. Kumar and A. K. Sikder, *Materials Science and Engineering: R: Reports*, 2004, **45**, 89-220.
14. G. Lim, J.-H. Lee, J. Kim, H.-W. Lee and S.-H. Hyun, *Materials Science Forum*, 2004, **449-452**, 1105-1108.
15. Z.-R. Tang, J. K. Edwards, J. K. Bartley, S. H. Taylor, A. F. Carley, A. A. Herzing, C. J. Kiely and G. J. Hutchings, *Journal of Catalysis*, 2007, **249**, 208-219.
16. T. Campbell Charles and H. F. Peden Charles, *Science*, 2005, **309**, 713-714.
17. *Application: WO Pat.,* 2002-GB5013 2003040270, 2003.
18. *Application: WO Pat.,* 2001-GB4777 2002034842, 2002.
19. E. P. Murray, T. Tsai and S. A. Barnett, *Nature (London)*, 1999, **400**, 649-651.
20. A. Ahniyaz, Y. Sakamoto and L. Bergström, *Crystal Growth & Design*, 2008, **8**, 1798-1800.
21. T. Masui, H. Hirai, N. Imanaka, G. Adachi, T. Sakata and H. Mori, *Journal of Materials Science Letters*, 2002, **21**, 489-491.
22. A. Sehgal, Y. Lalatonne, J. F. Berret and M. Morvan, *Langmuir*, 2005, **21**, 9359-9364.
23. G. K. Wertheim, J. H. Wernick and G. Crecelius, *Physical Review B*, 1978, **18**, 875-879.
24. B. Johansson, *Physical Review B*, 1979, **19**, 6615-6619.
25. E. Schweda and Z. Kang, eds. G. Adachi, N. Imanaka and Z. C. Kang, Springer Netherlands, 2005, pp. 57-93.
26. M. Auffan, J. Rose, C. Chanéac, J. P. Jolivet, A. Masion, M. R. Wiesner and J. Y. Bottero, *Nanoethics and Nanotoxicology*, 2011, 269.
27. T. Moeller, D. F. Martin, L. C. Thompson, R. Ferrús, G. R. Feistel and W. J. Randall, *Chemical Reviews*, 1965, **65**, 1-50.
28. K. L. Nash and M. P. Jensen, ed. . North-Holland Publishing Company, 2000, vol. 28, ch. 180, pp. 331-367.
29. G. R. Choppin, *Pure and Applied Chemistry*, 1971, **27**, 23-42.
30. R. G. Pearson, *Journal of the American Chemical Society*, 1963, **85**, 3533-3539.
31. G. R. Choppin and P. J. Wong, in *Coordination Chemistry*, American Chemical Society, 1994, vol. 565, ch. 29, pp. 346-360.
32. G. R. Choppin, *Thermochimica Acta*, 1993, **227**, 1-7.
33. G. R. Choppin and A. J. Graffeo, *Inorganic Chemistry*, 1965, **4**, 1254-1257.
34. G. R. Choppin and W. F. Strazik, *Inorganic Chemistry*, 1965, **4**, 1250-1254.
35. G. R. Choppin and S. L. Bertha, *Journal of Inorganic and Nuclear Chemistry*, 1973, **35**, 1309-1312.
36. G. R. Choppin, *Journal of the Less Common Metals*, 1984, **100**, 141-151.
37. G. R. Choppin, *Journal of Alloys and Compounds*, 1997, **249**, 9-13.
38. J. Huskens, H. van Bekkum, J. A. Peters and G. R. Choppin, *Inorganica Chimica Acta*, 1996, **245**, 51-57.
39. J. L. Bear, G. R. Choppin and J. V. Quagliano, *Journal of Inorganic and Nuclear Chemistry*, 1962, **24**, 1601-1606.
40. H. Diehl, *Chemical Reviews*, 1937, **21**, 39-111.
41. G. Schwarzenbach, *Helvetica Chimica Acta*, 1952, **35**, 2344-2359.
42. G. R. Choppin, *Journal of Alloys and Compounds*, 1997, **249**, 1-8.
43. T. F. Gritmon, M. P. Goedken and G. R. Choppin, *Journal of Inorganic and Nuclear Chemistry*, 1977, **39**, 2021-2023.
44. G. R. Choppin, M. P. Goedken and T. F. Gritmon, *Journal of Inorganic and Nuclear Chemistry*, 1977, **39**, 2025-2030.
45. F. A. Cotton and F. E. Harris, *The Journal of Physical Chemistry*, 1956, **60**, 1451-1454.
46. G. Anderegg, *Inorganica Chimica Acta*, 1980, **40**, X44.
47. Y. Gfeller and A. Merbach, *Inorganica Chimica Acta*, 1978, **29**, 217-225.
48. K. Nakamoto, *Infrared and Raman Spectra of Inorganic and Coordination Compounds, Applications in Coordination, Organometallic, and Bioinorganic Chemistry*, John Wiley & Sons, 1997.
49. P. A. Baisden, G. R. Choppin and B. B. Garrett, *Inorganic Chemistry*, 1977, **16**, 1367-1372.

RSC Advances Accepted Manuscript

50. N. V. Skorodumova, R. Ahuja, S. I. Simak, I. A. Abrikosov, B. Johansson and B. I. Lundqvist, *Physical Review B*, 2001, **64**, 115108.
51. L. R. Morss, in *Handbook on the Physics and Chemistry of Rare Earths*, eds. J. L. E. G. R. C. Karl A. Gschneidner and G. H. Lander, Elsevier, 1994, vol. Volume 18, pp. 239-291.
52. C. Binet, M. Daturi and J.-C. Lavalley, *Catalysis Today*, 1999, **50**, 207-225.
53. I. W. Siriwardane, Master's Thesis, University of Iowa, 2012.
54. M. Aguirre, M. Paulis and J. R. Leiza, *Journal of Materials Chemistry A*, 2013, **1**, 3155-3162.
55. J. M. Asua, *Journal of Polymer Science Part A: Polymer Chemistry*, 2004, **42**, 1025-1041.
56. M. J. Barandiaran, J. C. d. l. Cal and J. M. Asua, in *Polymer Reaction Engineering*, Blackwell Publishing Ltd, 2008, pp. 233-272.
57. Z. W. Wicks, F. N. Jones, S. P. Pappas and D. A. Wicks, *Organic Coatings: Science and Technology*, Wiley, 2007.

RSC Advances Accepted Manuscript